

Evidence of deviations between experimental and empirical mixing lengths: Multi-discharge field tests in an arid river system

Aashish Khandelwal ^a, Tzion Castillo ^{a,b}, Ricardo González-Pinzón ^{a,*}

^a Gerald May Department of Civil, Construction and Environmental Engineering, University of New Mexico, Albuquerque, NM USA

^b Electrical Engineering, University of New Mexico, Albuquerque, NM USA

ARTICLE INFO

Keywords:

Mixing length

Lagrangian

Wastewater treatment plant

Effluent

River mixing

ABSTRACT

Despite advances in wastewater treatment plant (WWTP) efficiencies, multiple contaminants of concern, such as microplastics, pharmaceuticals, and per- and poly-fluoroalkyl substances (PFAS) remain largely untreated near discharge points and can be highly concentrated before they are fully mixed within the receiving river. Environmental agencies enforce mixing zone permits for the temporary exceedance of water quality parameters beyond targeted control levels under the assumption that contaminants are well-mixed and diluted downstream of mixing lengths, which are typically quantified using empirical equations derived from one-dimensional transport models. Most of these equations were developed in the 1970s and have been assumed to be standard practice since then. However, their development and validation lacked the technological advances required to test them in the field and under changing flow conditions. While new monitoring techniques such as remote sensing and infrared imaging have been employed to visualize mixing lengths and test the validity of empirical equations, those methods cannot be easily repeated due to high costs or flight restrictions. We investigated the application of Lagrangian and Eulerian monitoring approaches to experimentally quantify mixing lengths downstream of a WWTP discharging into the Rio Grande near Albuquerque, New Mexico (USA). Our data spans river to WWTP discharges ranging between 2–22x, thus providing a unique dataset to test long-standing empirical equations in the field. Our results consistently show empirical equations could not describe our experimental mixing lengths. Specifically, while our experimental data revealed “bell-shaped” mixing lengths as a function of increasing river discharges, all empirical equations predicted monotonically increasing mixing lengths. Those mismatches between experimental and empirical mixing lengths are likely due to the existence of threshold processes defining mixing at different flow regimes, i.e., jet diffusion at low flows, the Coanda effect at intermediate flows, and turbulent mixing at higher flows, which are unaccounted for by the one-dimensional empirical formulas. Our results call for a review of the use of empirical mixing lengths in streams and rivers to avoid widespread exposures to emerging contaminants.

1. Introduction

Globally, large volumes of untreated and treated wastewater generated by domestic, industrial, and commercial sources are discharged into rivers, lakes, and marine systems, typically as point sources (Rice et al., 2013; UNESCO, 2020). According to the United Nations, the global volume of treated wastewater generated in 2018 was approximately 340 billion cubic meters, and it is projected to increase to 574 billion cubic meters by the year 2050 (United Nations Environment Programme, 2021). While technological advances have played a significant role in increasing the capacity to treat wastewater and improve

its quality (Angelakis and Snyder, 2015), multiple contaminants of concern, such as microplastics, pharmaceuticals, and per- and poly-fluoroalkyl substances (PFAS) remain largely untreated (Aymerich et al., 2017; Meng et al., 2020; Podder et al., 2021; Tiwari et al., 2017). Given the urgent need to increase water supply through water reuse of partially and fully treated wastewaters for landscaping (Baawain et al., 2020), irrigation (Mortensen et al., 2016), and human consumption (Mizyed, 2013), the interest in understanding environmental mixing, dilution, and overall wastewater management in fluvial systems is re-emerging (Antweiler et al., 2014; Aymerich et al., 2017; Kraus et al., 2017).

* Corresponding author.

E-mail address: gonzaric@unm.edu (R. González-Pinzón).

There are best practice guidelines for establishing mixing zones, i.e., areas where active mixing and dilution of effluents occur (EPA 305(b) report, 2009). In these mixing zones, pollutant concentrations can temporarily exceed water quality standards until contaminants are mixed and diluted by receiving water bodies. Near point sources, mixing zones are primarily influenced by the orientation of the outfall, its size, and the differences in flow and densities between the river and the effluent. Farther downstream, mixing is more influenced by the river's geomorphology (i.e., width, depth, sinuosity) and dilution capacity (Campos et al., 2022; Jirka et al., 1996). In practice, mixing zones (a 2D problem) are estimated through mixing lengths (1D approach) (Cooke et al., 2010), i.e., the distance downstream from a point source required to homogenize vertically and laterally solute concentrations in a receiving river (Rutherford, 1994). Even though most empirical mixing length equations have not been tested in the field with high-resolution techniques and under various flow conditions, they remain in use as standard practice.

The most commonly used empirical mixing length equations are derived from one-dimensional solute transport models, and while they include physical and hydraulic parameters describing the river's potential for dispersion and mixing through turbulence (Chapra, 2008; Cleasby and Dodge, 1999; Fischer, 1979; Jirka and Weitbrecht, 2005; Rup, 2006; Ward, 1973), they do not explicitly account for water temperature and density differences between the river and the effluent, even though temperature-related stratification affects mixing in lentic (e.g., lakes) and lotic systems (e.g., streams) (Gualtieri et al., 2019; Zavala, 2020). While not accounting for differences in temperatures and densities is appropriate in some practical estimations of mixing lengths, such as establishing sampling sites to collect data to model the 1D transport of a hydrologic tracer instantaneously injected (González-Pinzón et al., 2022), such differences are important in other relevant mixing problems involving fresh and saline waters (Haghnazari et al., 2022; Heiss and Michael, 2014), rivers draining watersheds with contrasting geochemistry (Gualtieri et al., 2019; Lane et al., 2008), and the discharge of wastewater treatment plant (WWTP) effluents in arid rivers. Since arid regions hold over one-third of the global population and half of the world's livestock and cultivated land (Millennium Ecosystem Assessment (Program), 2005), WWTP effluents may cause sustained and widespread water quality deterioration under drought conditions (Hur et al., 2007; Kamjunke et al., 2022; Mortensen et al., 2016). Therefore, correctly estimating mixing lengths becomes imperative to protect communities withdrawing water near WWTP effluents (Campos et al., 2022; Cleasby and Dodge, 1999).

Recent technological advances offer opportunities to test the validity of empirical mixing length equations. Remote sensing using satellite imagery can provide spatially distributed information on water quality parameters, including temperature, chlorophyll-a, and turbidity (Gholizadeh et al., 2016). However, satellite information's temporal and spatial resolutions are typically inadequate to support local-scale and dynamic decision-making for managing surface water resources. Drone-based infrared and photogrammetric surveys have also gained popularity as they provide better spatial resolution (Casas-Mulet et al., 2020; Dugdale et al., 2019; Pai et al., 2017). Still, short battery lives, low payload capacity, high costs, and overwhelming regulatory restrictions severely limit the area they can cover. An alternative to overcoming these challenges is using Lagrangian monitoring (i.e., as the flow goes) with high-resolution water quality sondes to detect where two distinct water sources become homogenous.

In this study, we quantified experimental mixing lengths downstream of a WWTP effluent in the Rio Grande near Albuquerque, New Mexico (USA), and compared our results against six commonly used empirical equations. We quantified experimental mixing lengths monitoring the two banks of the river using Lagrangian sampling with The Navigator (Khandelwal et al., 2023) and an instrumented kayak, and also used Eulerian monitoring across river transects when navigating the river was impossible due to low flows. Our experimental fieldwork was

done under six different river flow conditions, generating river-to-WWTP discharge ratios ranging from 2 to 22. Our study provided unique opportunities to investigate how mixing lengths vary as a function of flow dynamics in shallow, wide river reaches.

2. Methods

2.1. Study area

We studied a ~9 km reach of the Rio Grande near Albuquerque under six flow conditions ranging from $3.7 \text{ m}^3/\text{s}$ to $50.9 \text{ m}^3/\text{s}$, with a mean discharge of $16.7 \text{ m}^3/\text{s}$. This reach is located ~55 km downstream from Cochiti Lake, a large flood control reservoir maintained by the U.S. Army Corps of Engineers, and near the City of Albuquerque, where the treated effluent of the Southside Water Reclamation Plant is discharged. This wastewater treatment plant (WWTP) serves over 600,000 people and has an average daily effluent discharge of $2.6\text{--}3.2 \text{ m}^3/\text{s}$ (Brown and Caldwell, 2011). The WWTP outfall features a rock-lined channel merging into the left bank of the river at an angle of 45° . Our study reach starts 1.2 km upstream of the outfall of the WWTP and ends 7.8 km downstream of it.

The United States Geological Survey (USGS) operates gage USGS08330000 at Central Bridge, ~8.0 km upstream of the start of the reach, and gage USGS08330830 at Valle De Oro, ~4.7 km downstream of the outfall. We obtained discharge values from these gages upstream (Q_{up}) and downstream of the WWTP (Q_{down}). The Albuquerque Bernalillo County Water Utility Authority monitors the effluent coming from the WWTP, providing discharge (Q_{wwtp}) and water quality data at an hourly resolution (Fig. 1). The effluent from the WWTP is relatively constant with respect to the Rio Grande, and in some dry periods, it may make up most of the river (Fig. 2). In 2022, after more than 40% of the Rio Grande watershed experienced exceptional drought in early summer (Pratt, 2022), the WWTP effluent supplied all the discharge in the Rio Grande. Given that we covered dilution ratios $Q_{up} : Q_{wwtp}$ ranging between 2-22, our study design was ideal for investigating how mixing lengths vary as a function of flow in shallow, wide rivers.

2.2. Field Measurements

2.2.1. Infrared imagery

We used a drone equipped with a thermal imaging infrared camera (FLIR Vue Pro R 640) and an RGB camera (20 MP 1" CMOS) to visualize WWTP effluent and river water mixing with surface water temperature profiles. This fieldwork was completed on Nov 11, 2021, when $Q_{up} : Q_{wwtp} = 6.21$ (Fig. 3). Although the collected imagery was ideal for visualizing mixing patterns near the WWTP-river confluence, the technology only monitors temperature, is costly, and drone flying restrictions near the Albuquerque International Airport restricted its use in our area of interest. Thus, we only used the information collected from thermal imagery to design our Lagrangian and Eulerian monitoring.

2.2.2. High-resolution Lagrangian monitoring

We monitored the spatiotemporal variability of water quality parameters along the left and right banks of our study reach to characterize mixing lengths. These data were collected on the left bank using The Navigator, an autonomous surface vehicle instrumented with a GPS tracker and multiparameter sondes monitoring temperature, dissolved oxygen, pH, and specific conductivity at a depth of 0.2 m (Khandelwal et al., 2023). On the right bank, we used a kayak carrying a multiparameter YSI EXO2 sonde and a handheld GPS tracker to monitor the same parameters. The monitoring was completed under four different flow conditions, i.e., $Q_{up} : Q_{wwtp}$ of 5.5, 7.3, 12.5, and 22.1. On average, the data were collected at a spatial resolution of 72-102 m, over 2hr 16min - 3hr 48min of navigation.

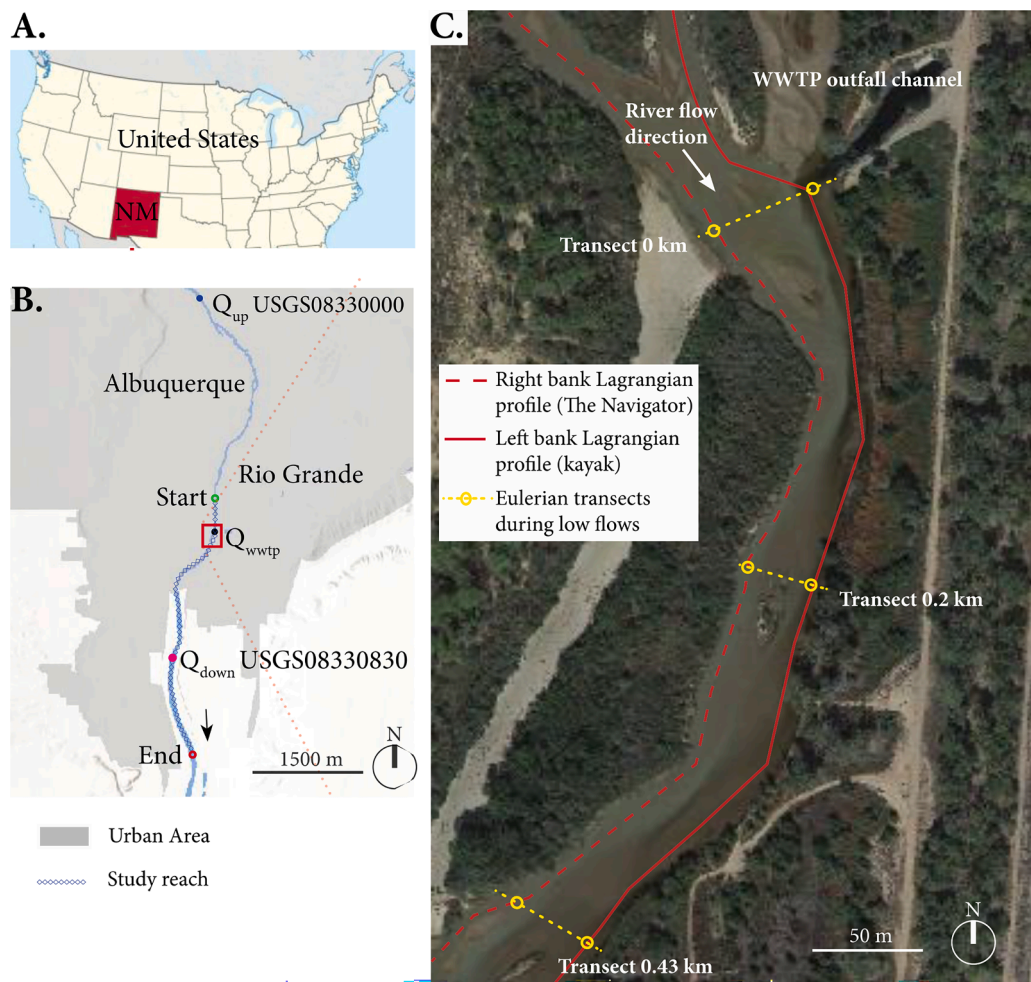


Fig. 1. (A and B) Study reach location and (C) satellite photo of the area near the outfall of the City of Albuquerque's wastewater treatment plant.

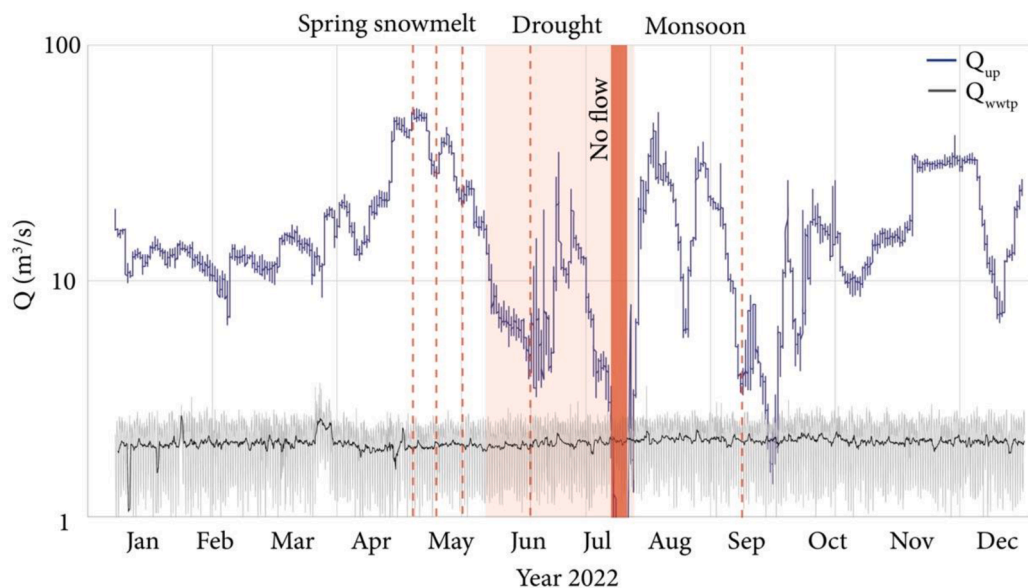


Fig. 2. Rio Grande discharge (blue) for the USGS08330000 at Central Bridge (Q_{up}), Southside Water Reclamation Plant outfall flow (Q_{wwtp} ; grey), and daily mean Q_{wwtp} values (black). Red dashed lines indicate fieldwork days, and the red rectangle represents the period when the river ran dry, and the WWTP provided all the river flow downstream of the WWTP.

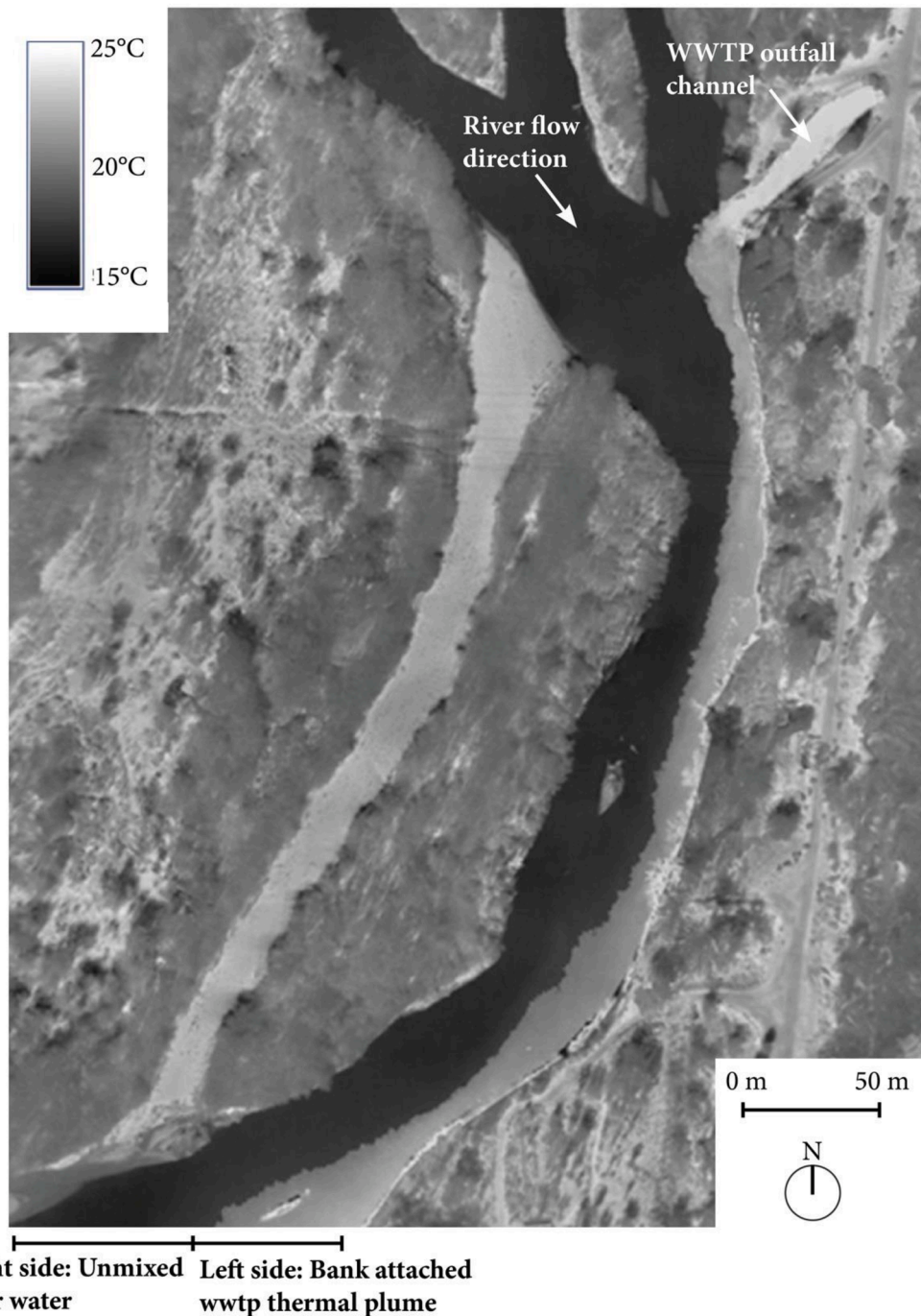


Fig. 3. Drone-based infrared imaging showing the higher temperature plume from the WWTP effluent (light grey, ~20–25 °C) hanging on the left bank of the Rio Grande (black, ~15 °C).

2.2.3. Eulerian monitoring:

In low flows with $Q_{up} : Q_{wwtp}$ of 2.4 and 3.6, we could not navigate the study reach and used Eulerian monitoring. We used the same multiparameter YSI EXO2 sondes along 11 transects spaced 200 m–2 km apart, depending on site access to the river. Before each Lagrangian or Eulerian monitoring field day, we calibrated each sensor following the manufacturer's recommendations.

2.3. Estimation of mixing lengths and comparison with existing models

We used sonde and GPS data to generate heatmaps of water quality parameters using the *spacetime* and *trajectories* package from R

(Pebesma, 2016). We estimated experimental mixing lengths (L_m) for each parameter as the distance required for left and right bank values to become $\pm 5\%$ equal or uniform downstream of the WWTP outfall (Fischer, 1979). Using this criterion, we confirmed that water quality parameter values upstream of the WWTP outfall were uniform.

The heatmaps (KMZ files) were arranged next to one other and imported into Google Earth to create layered displays of water quality data under different dilution ratios. The resolution of the Eulerian monitoring was increased using linear interpolation between transects to generate a higher-resolution heatmap.

We compared our experimental estimates of mixing lengths (L_m) with multiple empirical equations (L ; Table 1). The reach characteristics

Table 1
Empirical formulas used to compare mixing lengths.

Source	Equation
Mixing length zone (Fischer, 1979)	$L = \frac{kb^2 U}{Ru_*}$ (1)
Length of the longitudinal mixing zone (Rutherford, 1994)	$L = 0.536 \frac{Us^2}{D_y}$ (2)
Mixing length equation (Jirka and Weitbrecht, 2005; Skorbiłowicz et al., 2017)	$L = 0.4 \frac{Us^2}{D_y}$ (3)
Mixing length equation (Rup, 2006; Skorbiłowicz et al., 2017)	$L = 0.29 \frac{Us^2}{D_y}$ (4)
One half width mixing equation. (Cleasby and Dodge, 1999)	$L = \frac{0.4(b/2)^2 U}{D_y}$ (5)
European Union rule of thumb for river mixing zone. (Environmental Quality Standards, 2008)	$L = 10 b$ (6)

required to populate those equations include average velocity, depth, width, channel irregularity, and longitudinal slope values. The hydraulic parameters velocity, depth, and width were obtained from USGS data from the upstream station. Onsite observations of channel meandering and inspection of satellite imagery were used to determine a qualitative measure of channel irregularity (sinuosity) and longitudinal slopes.

In Table 1, L is the empirical mixing length, b is the channel width, U is the mean velocity, R is the hydraulic radius, u_* is the shear velocity, s is the linear transverse scale, D_y is the transverse dispersion coefficient ($D_y \sim 0.3 \text{ m}^2/\text{s}$ for the Rio Grande), and k is a channel type constant ($k \sim 10$ for the Rio Grande).

Through this consistent, repeatable, and comparable set of analyses spanning six dilution ratios ($2 < Q_{up} : Q_{wwtp} < 22$), and monitoring four traditional water quality parameters, we were able to compare experimental mixing lengths with respect to six empirical equations commonly used by practitioners and researchers.

3. Results and Discussion

3.1. Flow conditions and historical drought

The Rio Grande is a highly managed arid river system, providing water for 6 million people and irrigating 2 million acres of land. Drought years strain water operations, making flow management complex. Nearly 75% of the Rio Grande's water is used for agriculture, and managing low flows represent an environmental concern for endangered native species, particularly the Rio Grande Silvery Minnow (Pratt, 2022). In 2022, 40% of the Rio Grande watershed experienced exceptional drought, resulting in record-low flows during the summer and fall. Near Albuquerque, the river faced $\sim 19.5\%$ lower flows than the average flow since 1970. During the fieldwork days of this study, the river flow at Q_{up} ranged from $3.74 \text{ m}^3/\text{s}$ to $50.9 \text{ m}^3/\text{s}$, and the wastewater flow at Q_{wwtp} ranged from $1.56 \text{ m}^3/\text{s}$ to $3.01 \text{ m}^3/\text{s}$. These flow values generated dilution ratios between 2.4 - 22.1. Also, river depths ranged from 0.2 - 0.9 m (Table 2).

3.2. Experimental mixing lengths

The experimental mixing lengths observed from our datasets follow a

bell-shaped pattern with river flows and dilution ratios $Q_{up} : Q_{wwtp}$, i.e., low and high flows have smaller mixing lengths and intermediate flows have greater magnitudes (Figs. 4-6). Multiple mixing lengths were obtained from each water quality parameter tracked for a specific river flow or dilution ratio, even though they all followed the same bell-shaped patterns (Figs. 4-6). This suggests that contrasting phenomena at low and high flows may affect mixing length patterns similarly.

As river flows decrease, the outfall effluent has a higher depth and momentum, supporting a relatively fast and expansive mixing driven by kinetic energy in a process analogous to jet diffusion (Gomolka et al., 2022). The reduced river depth limits vertical spreading, causing the negatively buoyant effluent to rise rapidly, contributing to horizontal mixing (Pouchoulin et al., 2020). Additionally, the shallow depth of the river increases the relevance of shear stresses on stirring and mixing, enhancing the dispersion of the effluent and, thus, reducing mixing lengths (Chen et al., 2013).

We observed increased mixing lengths at intermediate river flows. Experimental observations with air and water have shown that fluids tend to remain attached to surfaces at increased flow velocities, a phenomenon known as the Coanda effect (Lalli et al., 2010). This attachment is due to pressure differences caused by differential flow velocities and contributes to "bank-hugging" of effluent plumes. Also, as river flows increase, river temperatures decrease, and the difference in water densities between the river and the WWTP increase, creating water stratification, which results in reduced mixing (Buxton et al., 2022; Elçi, 2008; Gualtieri et al., 2019; Lane et al., 2008). The EPA regulations under Clean Water Act recommend avoiding bank-hugging plumes or dominance of the Coanda effect in receiving water bodies that are used for irrigation, that host migrating and endangered fish, or where recreational activities can be impacted by non-mixing plumes (Clean Water Act Section 316(a), 2007).

At higher flows, mixing lengths consistently decreased due to increased turbulent mixing, which overcame the dominance of Coanda and water stratification effects (Campos et al., 2022). Since the wastewater temperature was consistently higher than that of the river, effluent plumes rose, contributing to faster vertical mixing. Combined with increased turbulent and vertical mixing, the higher dilution potential under high flows shortened mixing lengths (Lewis et al., 2020).

3.3. Experimental mixing lengths vs. empirical mixing lengths

We compared our experimental mixing lengths with the one-dimensional empirical equations from Table 1 (Fig. 6). Notably, none of the empirical equations can reproduce the bell-shaped mixing length pattern observed for all water quality parameters. Those empirical equations are monotonically increasing and vary from simple to intermediately complex considerations derived from one-dimensional transport models. Generally, the shortest mixing length prediction was obtained with Equation 6, which only uses width to predict mixing (Environmental Quality Standards, 2008), and the longest prediction was obtained with Equation 1 (Fischer, 1979) which accounts for shear stresses, unlike the others tested. Also, generally, the discrepancy between the predictions with empirical equations grew with river discharge, as all are proportional to flow velocity. In low flows with

Table 2
Hydrologic characteristics of the Rio Grande near Albuquerque, NM.

$\frac{Q_{up}}{Q_{wwtp}}$	$Q_{up} (\text{m}^3/\text{s})$	$Q_{wwtp} (\text{m}^3/\text{s})$	$Q_{down} (\text{m}^3/\text{s})$	Depth (m)	Width, b (m)	Area (m ²)	Hydraulic radius, R (m)	Mean velocity, U (m/s)	Linear transverse scale, s (m)
2.4	3.74	1.6	5.4	0.2	18	4	0.2	0.9	12.6
3.6	7.0	2.0	8.5	0.3	27	8	0.3	0.9	18.9
5.5	15.0	2.7	15.6	0.5	38	17	0.4	0.9	26.6
7.3	22.1	3.0	19.0	0.6	44	25	0.6	0.9	30.8
12.5	33.4	2.7	32.0	0.7	53	37	0.7	0.9	37.1
22.1	50.9	2.3	50.7	0.9	65	59	0.9	0.9	45.5

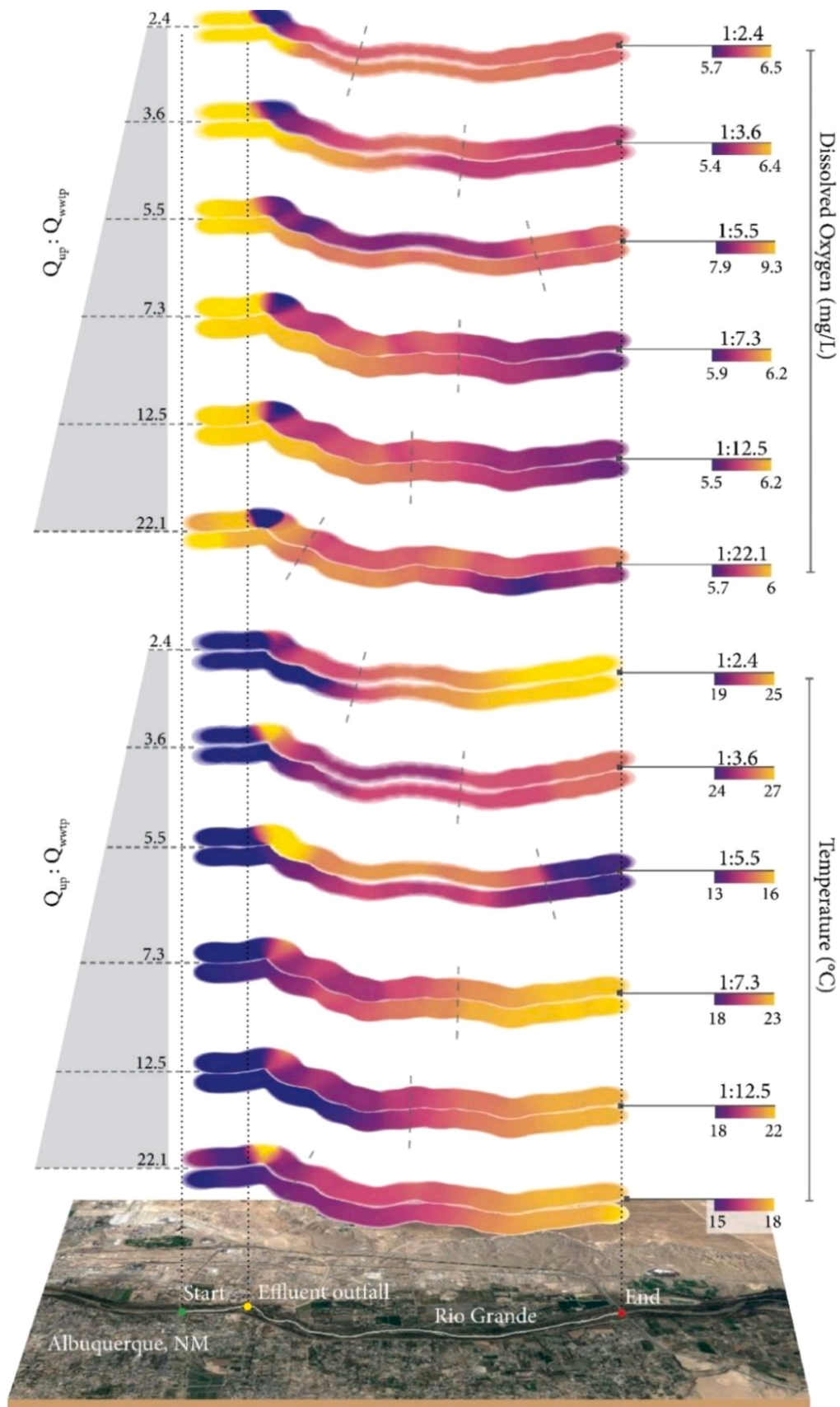


Fig. 4. Longitudinal profiles of dissolved oxygen and temperature observed upstream and downstream of the Albuquerque wastewater treatment plant (WWTP) effluent during different flow conditions ($Q_{up} : Q_{wwtp}$). Left bank (outfall side) data are on top of right bank data. Dash lines indicate the experimental mixing lengths (L_m), where left and right bank data are within 5% difference downstream of the WWTP.

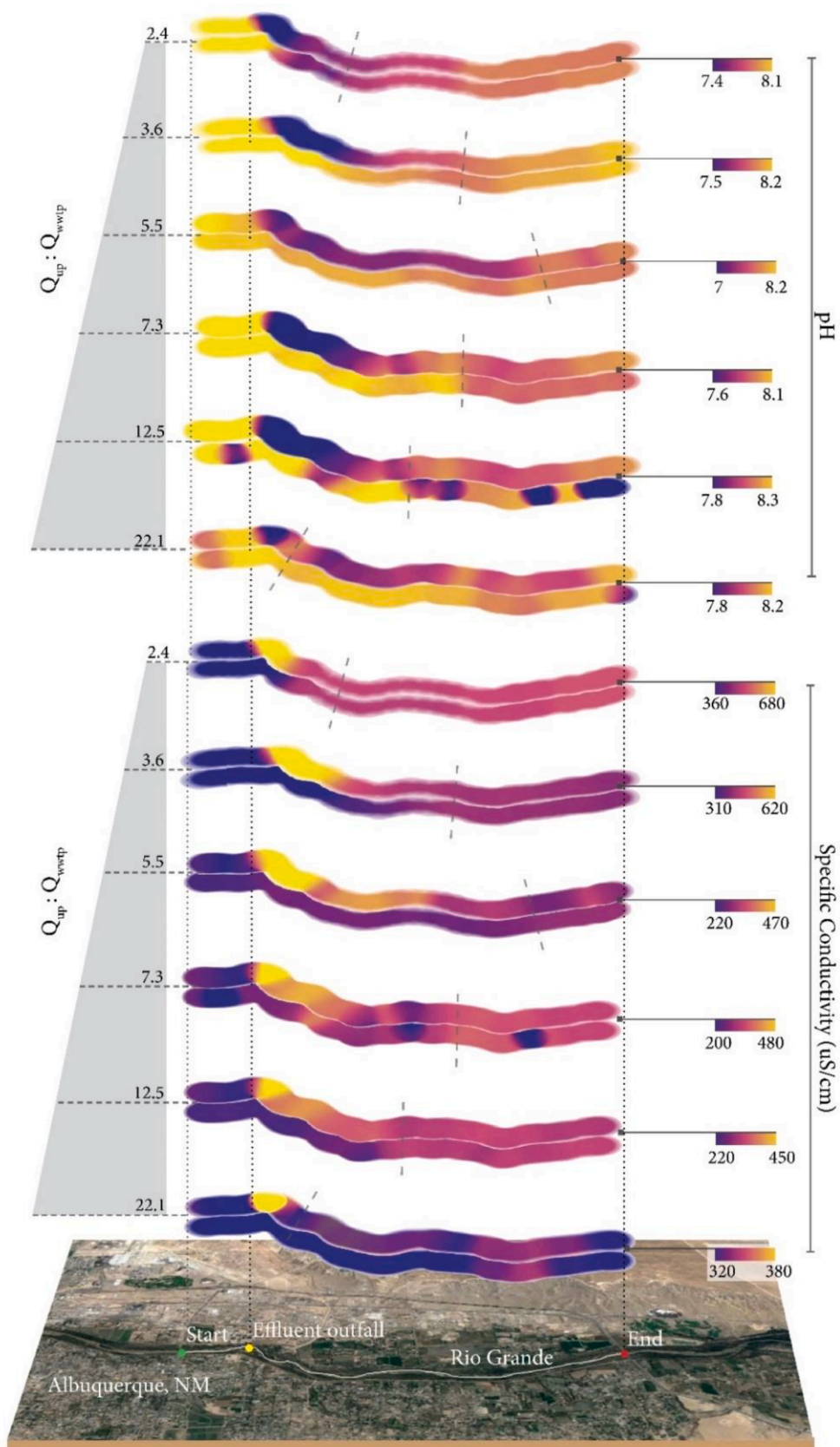


Fig. 5. Longitudinal profiles of pH and specific conductivity observed upstream and downstream of the Albuquerque wastewater treatment plant (WWTP) effluent during different flow conditions ($Q_{up} : Q_{wwtp}$). Left bank (outfall side) data are on top of right bank data. Dash lines indicate the experimental mixing lengths (L_m), where left and right bank data are within 5% difference downstream of the WWTP.

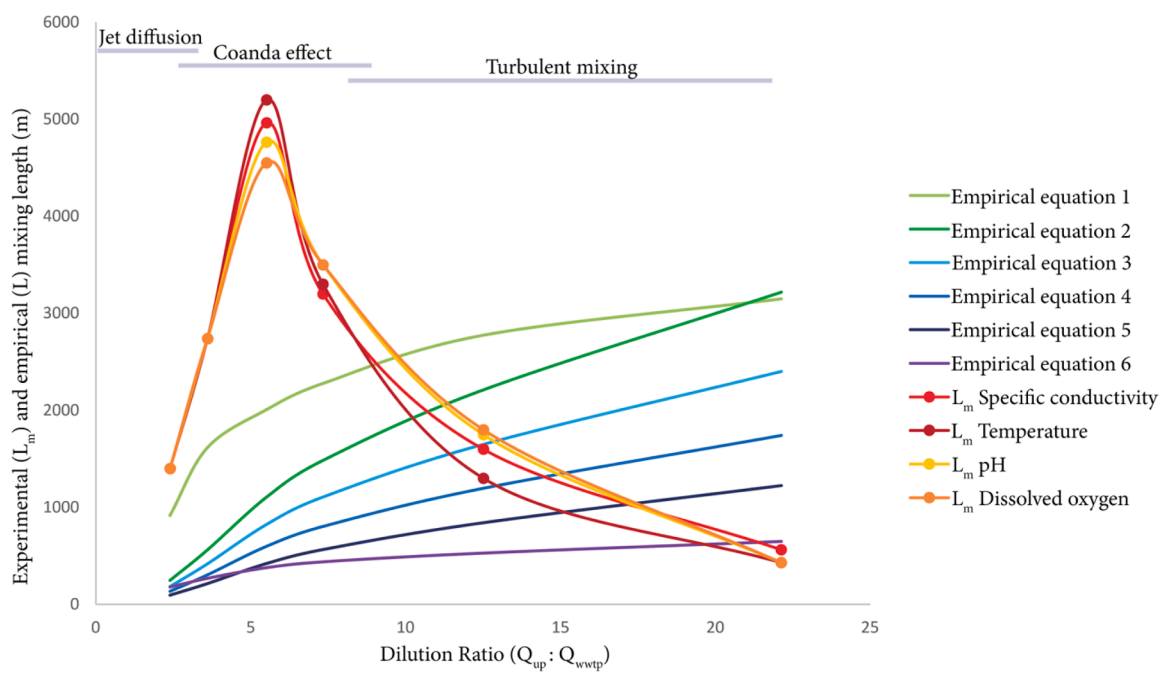


Fig. 6. Experimental (L_m) and empirical (L) mixing lengths as a function of the dilution ratio ($Q_{up} : Q_{wwtp}$). Empirical equations 1-6 are described in Table 1.

$2.4 < Q_{up} : Q_{wwtp} < 3.6$, our experimental mixing lengths were 1.5x to 7.5x longer than the predictions with empirical equations. In the intermediate flow region where the Coanda effect dominated, experimental mixing lengths were 2.5x-13x greater. In the highest $Q_{up} : Q_{wwtp} = 22.1$, experimental mixing lengths were 3x-7.5x smaller.

While empirical equations have found widespread use in engineering practice for analyzing mixing phenomena, their derivation disregarded complexities that may be relevant in real-world practice. For example, most equations assume straight channel geometries, uniform cross-sections, and steady flow conditions, disregarding the composition of bedforms and aquatic vegetation. However, streams and rivers undergo highly dynamic flow and sediment transport processes, making vertical, lateral, and longitudinal mixing highly dynamic. In this context, our field observations based on Lagrangian monitoring have revealed shifting mechanisms dominating mixing, i.e., jet diffusion, Coanda effect, and turbulent mixing (Fig. 6).

3.4. Advantages and limitations of estimating mixing lengths with high-resolution water quality parameters

Mixing in streams and rivers involves physical, biological, and chemical processes, which cooccur and influence one another (Hester et al., 2017; Jirka and Weitbrecht, 2005; Rutherford, 1994). Conservative substances or tracers are typically used to characterize physical transport processes (e.g., advection, dispersion, transient storage) because they are assumed to be effectively unaffected by biochemical reactions (e.g., decay or production) or state transformations (Divine and McDonnell, 2005; Emanuelson et al., 2022; González-Pinzón et al., 2022; Leibundgut et al., 2009). Despite these assumptions about their ideal behavior, biological and chemical processes still influence the transport of conservative substances. For example, biofilm growth can induce rate-limited mass-transfer processes between mobile (e.g., main channel) and less mobile (e.g., hyporheic or riparian) river zones, causing tailing in the transport of conservative substances (Battin et al., 2003; Bottacin-Busolin et al., 2009). Also, chemical stratification can delay or limit the mixing of conservative substances in rivers with contrasting densities (Gualtieri et al., 2019; Pouchoulin et al., 2020) and where dense (e.g., chlorinated solvents and some PFAS) and light (e.g., gasoline and pesticides) non-aqueous phase liquids are involved (Essaid

et al., 2015; Lyu et al., 2022). Consequently, compound-specific biochemical reactions should result in non-unique mixing length magnitudes, particularly in mixing problems involving point sources discharging a wide range of compounds (e.g., WWTP effluents). In this context, analyzing the advantages and limitations of using water quality parameters to estimate mixing lengths becomes practical, particularly because high-resolution sensors are revolutionizing hydrology and environmental engineering by allowing data collection efforts at high resolutions across spatial and temporal scales previously unattainable (Gabrielle, 2019; Griffiths et al., 2022; Nichols et al., 2022; Rode et al., 2016; Summers et al., 2020).

Our study monitored water quality parameters of environmental relevance efficiently and cost-effectively from two end members (i.e., WWTP effluent and upstream river) before and after they mixed. While biochemical processes could affect temperature, dissolved oxygen, pH, and specific conductivity at spatiotemporal scales relevant to our study, making them effectively non-conservative, the contrasting magnitudes of those parameter between end members allowed us to identify multiple experimental mixing lengths, over multiple discharges, and at spatiotemporal resolutions that other techniques would not have allowed. For example, using discrete sampling of compounds not removed by wastewater treatment (e.g., artificial sweeteners, pharmaceuticals, and PFAS) would have become cost-prohibitive at the same sampling frequencies and spatial coverages at which we collected sensor-based water quality data. Similarly, the continuous injection of conservative tracers such as salts or dyes over multiple hours at our study site would have restricted the range of dilution ratios $Q_{up} : Q_{WWTP}$ that we could have explored due to logistical limitations associated with tracer costs, pumping costs, and the increased personnel needed.

Considering the advantages and limitations of using high-resolution water quality data from sondes to estimate experimental mixing lengths, the consistent bell-shaped mixing pattern observed with respect to discharge for four water quality parameters with varying degrees of non-conservativeness provides evidence to challenge the validity of empirical mixing length equations commonly used, particularly because they all systematically failed at capturing experimental patterns.

3.5. Impacts of mixing lengths on ecosystem services

Mixing lengths are relevant in water quality assessments and studies of ecosystem dynamics in streams and rivers. In water resources management, mixing lengths help assess risk and mitigation strategies that communities downstream of point and distributed sources should have to reduce pollution exposure when streams or rivers are used for irrigation, fishing, ceremonial uses, groundwater recharge, and drinking water purposes. Regions located between a contaminant source and the mixing length are prone to undergo pollution issues as water properties (e.g., temperature, solutes, and sediments) are not homogenized and could overwhelm ecosystems (Campos et al., 2022; Skorbiowicz et al., 2017).

In most cases, the effluent discharged from a WWTP contains higher levels of contaminants than the receiving stream or river, which can negatively impact ecosystem health and functioning (Castellar et al., 2022; Martí et al., 2009; Pascual-Benito et al., 2020). For example, the slow mixing of warmer plumes from WWTP can lead to reduced oxygen

levels, impacting fish communities (Caissie, 2006; Isaak et al., 2010; Perkins et al., 2012). Also, concentrated pharmaceutical and personal care products can be toxic to fish, amphibians, and invertebrates, disrupting hormone systems, impairing reproductive functions, and causing behavioral changes in these organisms (Adegoke et al., 2023; Ding et al., 2022; Hernando et al., 2006; Issac and Kandasubramanian, 2021; Wang et al., 2021).

While longer mixing length predictions generate more conservative and cautious estimates to help protect downstream water users, our results indicate that commonly used empirical equations may consistently underpredict mixing lengths in intermediate flow regimes, where the Coanda effect controls mixing. This underprediction could result in higher pollution risks for human populations capturing water from the same bank of upstream effluent discharges.

Beyond providing evidence to support the call for a review of the use of empirical mixing lengths in river systems, our study site also provides a window to observe why improving the prediction and application of mixing lengths matter to communities. Only 13 km downstream of the



Fig. 7. A) The effluent outfall of the City of Albuquerque's wastewater treatment plant is located on the left bank of the Rio Grande. In some drought years, the effluent can make all the river flow. B) 13 km downstream, the Isleta Diversion Dam diverts between ~50% (wet year) to ~100% (dry year) of the Rio Grande flow for irrigation, and one of the intakes is on the same side of the effluent outfall. Satellite images from Google Earth.

Albuquerque WWTP's outfall, which treats $\sim 227,000\text{-}273,000\text{ m}^3/\text{day}$ (i.e., 50-60 million gallons per day) of wastewater from $\sim 600,000$ users and discharges on the left bank of the Rio Grande, the Middle Rio Grande Conservancy District diverts water from both banks of the Rio Grande during the growing season through Isleta Diversion Dam (Fig. 7). Since 50%-100% of the Rio Grande flow can be typically diverted in wet and dry years, respectively (Oelsner et al., 2007), and the WWTP effluent can make up the total flow in the river (Fig. 2), all the effluent discharged may be diverted through the irrigation intake located on the left bank. Even though we observed experimental mixing lengths of $< 6\text{ km}$ (Fig. 6), when the Rio Grande runs dry or very low, most of the water flowing is WWTP effluent, which may carry highly concentrated microplastics, pharmaceuticals, and PFAS.

Besides water quality issues, relatively high-velocity effluents discharging from WWTPs may cause erosion problems, which, over time, can destabilize riverbanks and change the river's geomorphology (Duró et al., 2020). Between 1996-2023, the erosion occurring near the Albuquerque WWTP's outfall resulted in a $\sim 9400\text{ m}^2$ area lost on the left bank side (Fig. 8), affecting vegetation recruitment, which promotes even more erosion. To tackle these long-standing problems, the City of Albuquerque initiated a \$4.7 million restoration project in 2022 to realign the outfall, facilitate mixing with river water during low flow conditions, and restore crucial habitats for endangered fish and birds (Davis, 2022). For that, the restoration project used root wads, which are clusters consisting of logs, roots, and boulders strategically placed along the riverbank to create suitable fish habitats and mitigate streambed erosion. It is worth noting that the bank upstream of the outfall has exhibited consistent vegetation cover over the same period.

4. Conclusions

Using high-resolution Lagrangian and Eulerian monitoring, we assessed the impact of flow dynamics on mixing lengths downstream of a WWTP effluent discharge in the Rio Grande near Albuquerque, NM. The Lagrangian reference frame was critical to visualizing mixing lengths from the perspective of four different water quality parameters (i.e., dissolved oxygen, temperature, pH, and specific conductivity). The Eulerian reference frame allowed us to continue our experimental work under the extremely low flow conditions that halted our use of Lagrangian equipment flowing down the river. Both Lagrangian and Eulerian monitoring designs were initially informed by infrared imagery. Our results show that the empirical equations traditionally used to estimate mixing lengths did not describe our experimental dataset correctly and call for a review of the use of empirical mixing lengths in streams and rivers. While our experimental data revealed "bell-shaped" mixing lengths as a function of river:WWTP discharges, all empirical equations predicted monotonically increasing mixing lengths. Those mismatches between experimental and empirical mixing lengths are likely due to the existence of threshold processes defining mixing at different flow regimes, i.e., jet diffusion at low flows, the Coanda effect at intermediate flows, and turbulent mixing at higher flows, which are unaccounted for by the one-dimensional empirical formulas.

The successful use of The Navigator and an instrumented kayak (we had only built one prototype of The Navigator) to monitor both banks of the Rio Grande and test empirical equations commonly used in a problem long-thought to be well understood calls for increased use of Lagrangian monitoring to understand environmental dynamics better. With the advent of real-time telemetry and high-resolution sensors, Lagrangian monitoring can rapidly and cost-effectively generate datasets to connect better the impact of sources (e.g., spills, wildfire-affected

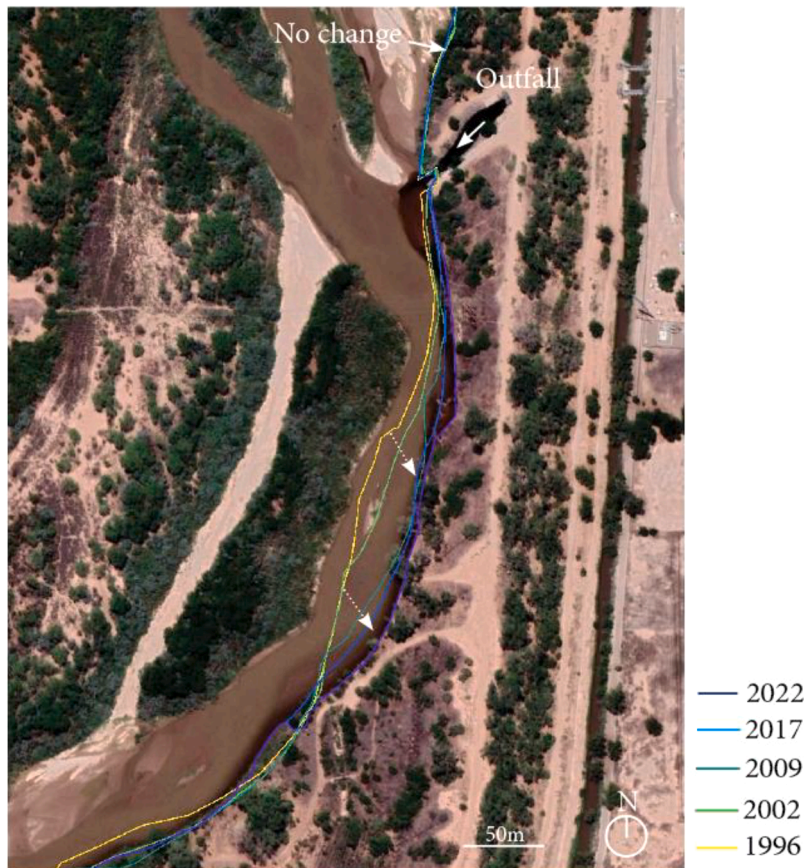


Fig. 8. Bankline evolution downstream of the Albuquerque WWTP outfall. The bank history has been obtained with satellite images from Google Earth.

watersheds, outfalls) on downstream communities. Our findings also highlight the importance of combining Eulerian and Lagrangian efforts to provide a more robust understanding of the dynamics of mass and energy fluxes and how they affect coupled human-environment systems.

Declaration of Competing Interest

Ricardo González-Pinzón reports financial support was provided by the National Science Foundation and the New Mexico Water Resources Research Institute.

CRediT authorship contribution statement

Aashish Khandelwal: Writing – review & editing, Writing – original draft, Software, Methodology, Investigation, Formal analysis, Data curation, Conceptualization. **Tzion Castillo:** Writing – review & editing, Validation, Methodology, Data curation. **Ricardo González-Pinzón:** Writing – review & editing, Writing – original draft, Validation, Supervision, Resources, Project administration, Methodology, Investigation, Funding acquisition, Formal analysis, Conceptualization.

Declaration of competing interest

The authors declare the following financial interests/personal relationships which may be considered as potential competing interests:

Ricardo Gonzalez-Pinzon reports financial support was provided by National Science Foundation.

Data availability

Data will be made available on request.

Acknowledgments

The National Science Foundation supported this research through grants EAR-2142691 and HRD-1914490. The New Mexico Water Resources Research Institute also supported this research. We thank David Van Horn, Stefan Krause, and Mark Stone for providing feedback on early versions of this manuscript.

References

Adegoke, K.A., Adu, F.A., Oyebamiji, A.K., Bamisaye, A., Adigun, R.A., Olasoji, S.O., Ogunjimi, O.E., 2023. Microplastics toxicity, detection, and removal from water/wastewater. *Marine Pollution Bulletin* 187, 114546. <https://doi.org/10.1016/j.marpolbul.2022.114546>.

Angelakis, A.N., Snyder, S.A., 2015. Wastewater Treatment and Reuse: Past, Present, and Future. *Water* 7, 4887–4895. <https://doi.org/10.3390/w7094887>.

Antweiler, R.C., Writer, J.H., Murphy, S.F., 2014. Evaluation of wastewater contaminant transport in surface waters using verified Lagrangian sampling. *Science of The Total Environment* 470–471, 551–558. <https://doi.org/10.1016/j.scitotenv.2013.09.079>.

Aymerich, I., Acuña, V., Ort, C., Rodríguez-Roda, I., Corominas, Ll., 2017. Fate of organic microcontaminants in wastewater treatment and river systems: An uncertainty assessment in view of sampling strategy, and compound consumption rate and degradability. *Water Research* 125, 152–161. <https://doi.org/10.1016/j.watres.2017.08.011>.

Baawain, M.S., Al-Mamun, A., Omidvarborna, H., Al-Sabti, A., Choudri, B.S., 2020. Public perceptions of reusing treated wastewater for urban and industrial applications: challenges and opportunities. *Environ Dev Sustain* 22, 1859–1871. <https://doi.org/10.1007/s10668-018-0266-0>.

Battin, T.J., Kaplan, L.A., Denis Newbold, J., Hansen, C.M.E., 2003. Contributions of microbial biofilms to ecosystem processes in stream mesocosms. *Nature* 426, 439–442. <https://doi.org/10.1038/nature02152>.

Bottacin-Busolin, A., Singer, G., Zaramella, M., Battin, T.J., Marion, A., 2009. Effects of Streambed Morphology and Biofilm Growth on the Transient Storage of Solutes. *Environmental Science & Technology* 43, 7337–7342. <https://doi.org/10.1021/es900852w>.

Brown and Caldwell, 2011. Open-File Report.

Buxton, T.H., Lai, Y.G., Som, N.A., Peterson, E., Abban, B., 2022. The mechanics of diurnal thermal stratification in river pools: Implications for water management and species conservation. *Hydrological Processes* 36, e14749. <https://doi.org/10.1002/hyp.14749>.

Caissie, D., 2006. The thermal regime of rivers: a review. *Freshwater Biology* 51, 1389–1406. <https://doi.org/10.1111/j.1365-2427.2006.01597.x>.

Campos, C.J.A., Morrisey, D.J., Barter, P., 2022. Principles and Technical Application of Mixing Zones for Wastewater Discharges to Freshwater and Marine Environments. *Water* 14, 1201. <https://doi.org/10.3390/w14081201>.

Casas-Mulet, R., Pander, J., Ryu, D., Stewardson, M.J., Geist, J., 2020. Unmanned Aerial Vehicle (UAV)-Based Thermal Infra-Red (TIR) and Optical Imagery Reveals Multi-Spatial Scale Controls of Cold-Water Areas Over a Groundwater-Dominated Riverscape. *Front. Environ. Sci.* 8 <https://doi.org/10.3389/fenvs.2020.00064>.

Castelar, S., Bernal, S., Ribot, M., Merbt, S.N., Tobella, M., Sabater, F., Ledesma, J.L.J., Guasch, H., Lupon, A., Gacia, E., Drummond, J.D., Martí, E., 2022. Wastewater treatment plant effluent inputs influence the temporal variability of nutrient uptake in an intermittent stream. *Urban Ecosyst* 25, 1313–1326. <https://doi.org/10.1007/s11252-022-01228-5>.

Chapra, S.C., 2008. *Surface Water-Quality Modeling*. Waveland Pr Inc, Long Grove, Ill.

Chen, X., Dong, W., Ou, G., Wang, Z., Liu, C., 2013. Gaining and losing stream reaches have opposite hydraulic conductivity distribution patterns. *Hydrology and Earth System Sciences* 17, 2569–2579. <https://doi.org/10.5194/hess-17-2569-2013>.

Clean Water Act Section 316(a), 2007. Point sources with thermal discharges.

Cleasby, T., Dodge, K., 1999. Effluent mixing characteristics below four wastewater-treatment facilities in southwestern Montana 1997. <https://doi.org/10.3133/wri994026>.

Cooke, J., Rutherford, K., Milne, P., 2010. A Review of Definitions of “Mixing Zones” and “Reasonable Mixing” in Receiving Waters.

Davis, T., 2022. Water authority project aims to excavate, realign South Valley wastewater outfall site - Albuquerque Journal [WWW Document]. URL <https://www.abqjournal.com/2525297/utility-will-restore-south-valley-wastewater-outfall-site.html> (accessed 5.24.23).

Ding, T., Wei, L., Hou, Z., Li, J., Zhang, C., Lin, D., 2022. Microplastics altered contaminant behavior and toxicity in natural waters. *Journal of Hazardous Materials* 425, 127908. <https://doi.org/10.1016/j.jhazmat.2021.127908>.

Divine, C.E., McDonnell, J.J., 2005. The future of applied tracers in hydrogeology. *Hydrogeol J* 13, 255–258. <https://doi.org/10.1007/s10040-004-0416-3>.

Dugdale, S.J., Kelleher, C.A., Malcolm, I.A., Caldwell, S., Hannah, D.M., 2019. Assessing the potential of drone-based thermal infrared imagery for quantifying river temperature heterogeneity. *Hydrological Processes* 33, 1152–1163. <https://doi.org/10.1002/hyp.13395>.

Duro, G., Crosato, A., Kleinhans, M.G., Winkels, T.G., Woolderink, H.A.G., Uijttewaal, W.S.J., 2020. Distinct patterns of bank erosion in a navigable regulated river. *Earth Surface Processes and Landforms* 45, 361–374. <https://doi.org/10.1002/esp.4736>.

Elçi, S., 2008. Effects of thermal stratification and mixing on reservoir water quality. *Limnology* 9, 135–142. <https://doi.org/10.1007/s10201-008-0240-x>.

Emanuelson, K., Covino, T., Ward, A.S., Dorley, J., Gooseff, M., 2022. Conservative solute transport processes and associated transient storage mechanisms: Comparing streams with contrasting channel morphologies, land use and land cover. *Hydrological Processes* 36, e14564. <https://doi.org/10.1002/hyp.14564>.

Environmental Quality Standards, 2008. *Technical Background Document on Identification of Mixing Zones*.

EPA 305(b) report, 2009. National Water Quality Inventory Report to Congress | Water Data and Tools | US EPA [WWW Document]. URL <https://www.epa.gov/waterdata/national-water-quality-inventory-report-congress> (accessed 9.26.19).

Essaid, H.I., Bekins, B.A., Cozzarelli, I.M., 2015. Organic contaminant transport and fate in the subsurface: Evolution of knowledge and understanding. *Water Resources Research* 51, 4861–4902. <https://doi.org/10.1002/2015WR017121>.

Fischer, H., 1979. *Mixing In Inland & Coastal Waters*: Hugo Fischer: Hardcover: 9780122581502: Powell's Books [WWW Document]. URL <https://www.powells.com/book/mixing-in-inland-coastal-waters-9780122581502> (accessed 3.10.22).

Gabrielle, V., 2019. The Renaissance of Hydrology [WWW Document]. Eos. URL <https://eos.org/features/the-renaissance-of-hydrology> (accessed 4.17.19).

Gholizadeh, M., Melesse, A., Reddi, L., 2016. A Comprehensive Review on Water Quality Parameters Estimation Using Remote Sensing Techniques. *Sensors* 16, 1298. <https://doi.org/10.3390/s16081298>.

Gomolka, Z., Twarog, B., Zeslawska, E., 2022. State Analysis of the Water Quality in Rivers in Consideration of Diffusion Phenomenon. *Applied Sciences* 12, 1549. <https://doi.org/10.3390/app12031549>.

González-Pinzón, R., Dorley, J., Singley, J., Singha, K., Gooseff, M., Covino, T., 2022. TIPT: The Tracer Injection Planning Tool. *Environmental Modelling & Software* 156, 105504. <https://doi.org/10.1016/j.envsoft.2022.105504>.

Griffiths, N.A., Levi, P.S., Riggs, J.S., DeRolph, C.R., Fortner, A.M., Richards, J.K., 2022. Sensor-Equipped Unmanned Surface Vehicle for High-Resolution Mapping of Water Quality in Low- to Mid-Order Streams. *ACS EST Water* 2, 425–435. <https://doi.org/10.1021/acs.estwater.1c00342>.

Gualtieri, C., Ianniruberto, M., Filizola, N., 2019. On the mixing of rivers with a difference in density: The case of the Negro/Solimões confluence. *Brazil. Journal of Hydrology* 578, 124029. <https://doi.org/10.1016/j.jhydrol.2019.124029>.

Haghnazari, H., Johannesson, K.H., González-Pinzón, R., Pourakbar, M., Aghayani, E., Rajabi, A., Hashemi, A.A., 2022. Groundwater geochemistry, quality, and pollution of the largest lake basin in the Middle East: Comparison of PMF and PCA-MLR receptor models and application of the source-oriented HHRA approach. *Chemosphere* 288, 132489. <https://doi.org/10.1016/j.chemosphere.2021.132489>.

Heiss, J.W., Michael, H.A., 2014. Saltwater-freshwater mixing dynamics in a sandy beach aquifer over tidal, spring-neap, and seasonal cycles. *Water Resources Research* 50, 6747–6766. <https://doi.org/10.1002/2014WR015574>.

Hernando, M., Mezcuia, M., Fernandezalba, A., Barcelo, D., 2006. Environmental risk assessment of pharmaceutical residues in wastewater effluents, surface waters and sediments. *Talanta* 69, 334–342. <https://doi.org/10.1016/j.talanta.2005.09.037>.

Hester, E.T., Cardenas, M.B., Haggerty, R., Apte, S.V., 2017. The importance and challenge of hyporheic mixing. *Water Resources Research* 53, 3565–3575. <https://doi.org/10.1002/2016WR020005>.

Hur, J., Schlautman, M.A., Karanfil, T., Smink, J., Song, H., Klaine, S.J., Hayes, J.C., 2007. Influence of Drought and Municipal Sewage Effluents on the Baseflow Water Chemistry of an Upper Piedmont River. *Environ Monit Assess* 132, 171–187. <https://doi.org/10.1007/s10661-006-9513-1>.

Isaak, D.J., Luce, C.H., Rieman, B.E., Nagel, D.E., Peterson, E.E., Horan, D.L., Parkes, S., Chandler, G.L., 2010. Effects of climate change and wildfire on stream temperatures and salmonid thermal habitat in a mountain river network. *Ecol Appl* 20, 1350–1371.

Issac, M.N., Kandasubramanian, B., 2021. Effect of microplastics in water and aquatic systems. *Environ Sci Pollut Res* 28, 19544–19562. <https://doi.org/10.1007/s11356-021-13184-2>.

Jirkka, G., Weitbrecht, V., 2005. Mixing Models for Water Quality Management in Rivers: Continuous and Instantaneous Pollutant Releases. *Water Quality Hazards and Dispersion of Pollutants* 1–34. https://doi.org/10.1007/0-387-23322-9_1.

Jirkka, G.H., Doneker, R.L., Hinton, S.W., 1996. USER'S MANUAL FOR CORMIX [1996].

Kamjunke, N., Beckers, L.-M., Herzsprung, P., von Tümpeling, W., Lechtenfeld, O., Tittel, J., Risse-Bühl, U., Rode, M., Wachholz, A., Kallies, R., Schulze, T., Krauss, M., Brack, W., Comero, S., Gawlik, B.M., Skejo, H., Tavazzi, S., Mariani, G., Borchardt, D., Weitere, M., 2022. Lagrangian profiles of riverine autotrophy, organic matter transformation, and micropollutants at extreme drought. *Science of the Total Environment* 828, 154243. <https://doi.org/10.1016/j.scitotenv.2022.154243>.

Khandelwal, A., Castillo, T., González-Pinzón, R., 2023. Development of The Navigator: A Lagrangian sensing system to characterize surface freshwater ecosystems. *Water Research* 120577. <https://doi.org/10.1016/j.watres.2023.120577>.

Kraus, T.E.C., Carpenter, K., Bergamaschi, B., Parker, A., Stumpner, E., Downing, B.D., Travis, N., Wilkerson, F., Kendall, C., Mussen, T., 2017. A river-scale Lagrangian experiment examining controls on phytoplankton dynamics in the presence and absence of treated wastewater effluent high in ammonium. *Limnology and Oceanography*. <https://doi.org/10.1002/lno.10497>.

Lalli, F., Bruschi, A., Lama, R., Liberti, L., Mandrone, S., Pesarino, V., 2010. Coanda effect in coastal flows. *Coastal Engineering* 57, 278–289. <https://doi.org/10.1016/j.coastaleng.2009.10.015>.

Lane, S.N., Parsons, D.R., Best, J.L., Orfeo, O., Kostaschuk, R.A., Hardy, R.J., 2008. Causes of rapid mixing at a junction of two large rivers: Río Paraná and Río Paraguay. *Argentine Journal of Geophysical Research: Earth Surface* 113. <https://doi.org/10.1029/2006JF000745>.

Leibundgut, C., Maloszewski, P., Külls, C., 2009. *Tracers in Hydrology* | Wiley. John Wiley & Sons, Ltd.

Lewis, Q., Rhoads, B., Sukhodolov, A., Constantinescu, G., 2020. Advective Lateral Transport of Streamwise Momentum Governs Mixing at Small River Confluences. *Water Resources Research* 56, e2019WR026817. <https://doi.org/10.1029/2019WR026817>.

Lyu, X., Xiao, F., Shen, C., Chen, J., Park, C.M., Sun, Y., Flury, M., Wang, D., 2022. Per- and Polyfluoroalkyl Substances (PFAS) in Subsurface Environments: Occurrence, Fate, Transport, and Research Prospect. *Reviews of Geophysics* 60, e2021RG000765. <https://doi.org/10.1029/2021RG000765>.

Marti, E., Riera, J.L., Sabater, F., 2009. Effects of Wastewater Treatment Plants on Stream Nutrient Dynamics Under Water Scarcity Conditions. In: Sabater, S., Barceló, D. (Eds.), *Water Scarcity in the Mediterranean, The Handbook of Environmental Chemistry*. Springer Berlin Heidelberg, Berlin, Heidelberg, pp. 173–195. https://doi.org/10.1007/698_2009_33.

Meng, Y., Kelly, F.J., Wright, S.L., 2020. Advances and challenges of microplastic pollution in freshwater ecosystems: A UK perspective. *Environmental Pollution* 256, 113445. <https://doi.org/10.1016/j.envpol.2019.113445>.

Millennium Ecosystem Assessment (Program) (Ed.), 2005. *Ecosystems and human well-being: synthesis*. Island Press, Washington, DC.

Mizyed, N.R., 2013. Challenges to treated wastewater reuse in arid and semi-arid areas. *Environmental Science & Policy* 25, 186–195. <https://doi.org/10.1016/j.envsci.2012.10.016>.

Mortensen, J.G., González-Pinzón, R., Dahm, C.N., Wang, J., Zeglin, L.H., Van Horn, D.J., 2016. Advancing the Food-Energy-Water Nexus: Closing Nutrient Loops in Arid River Corridors. *Environ. Sci. Technol.* 50, 8485–8496. <https://doi.org/10.1021/acs.est.6b01351>.

Nichols, J., Khandelwal, A.S., Regier, P., Summers, B., Van Horn, D.J., González-Pinzón, R., 2022. The understudied winter: Evidence of how precipitation differences affect stream metabolism in a headwater. *Front. Water* 4, 1003159. <https://doi.org/10.3389/frwa.2022.1003159>.

Oelsner, G.P., Brooks, P.D., Hogan, J.F., 2007. Nitrogen Sources and Sinks Within the Middle Rio Grande, New Mexico1. *JAWRA Journal of the American Water Resources Association* 43, 850–863. <https://doi.org/10.1111/j.1752-1688.2007.00071.x>.

Pai, H., Malenda, H.F., Briggs, M.A., Singha, K., González-Pinzón, R., Goosseff, M.N., Tyler, S.W., Team, the AirCTEMPS, 2017. Potential for Small Unmanned Aircraft Systems Applications for Identifying Groundwater-Surface Water Exchange in a Meandering River Reach. *Geophysical Research Letters* 44. <https://doi.org/10.1002/2017GL075836>.

Pascual-Benito, M., Nadal-Sala, D., Tobella, M., Balleste, E., García-Aljaro, C., Sabaté, S., Sabater, F., Martí, E., Gracia, C.A., Blanch, A.R., Lucena, F., 2020. Modelling the seasonal impacts of a wastewater treatment plant on water quality in a Mediterranean stream using microbial indicators. *Journal of Environmental Management* 261, 110220. <https://doi.org/10.1016/j.jenvman.2020.110220>.

Pebesma, E., 2016. Handling and Analyzing Spatial, Spatiotemporal and Movement Data [WWW Document]. URL <https://edzer.github.io/UseR2016/#spatiotemporal-data-movement-data> (accessed 1.18.23).

Perkins, D.M., Yvon-Durocher, G., Demars, B.O.L., Reiss, J., Pichler, D.E., Friberg, N., Trimmer, M., Woodward, G., 2012. Consistent temperature dependence of respiration across ecosystems contrasting in thermal history. *Glob Change Biol* 18, 1300–1311. <https://doi.org/10.1111/j.1365-2486.2011.02597.x>.

Podder, A., Sadmani, A.H.M.A., Reinhart, D., Chang, N.-B., Goel, R., 2021. Per and polyfluoroalkyl substances (PFAS) as a contaminant of emerging concern in surface water: A transboundary review of their occurrences and toxicity effects. *Journal of Hazardous Materials* 419, 126361. <https://doi.org/10.1016/j.jhazmat.2021.126361>.

Pouchoulin, S., Le Coz, J., Mignot, E., Gond, L., Riviere, N., 2020. Predicting Transverse Mixing Efficiency Downstream of a River Confluence. *Water Resour. Res.* 56 <https://doi.org/10.1029/2019WR026367>.

Pratt, S., 2022. Rio Grande Runs Dry, Then Wet [WWW Document]. URL <https://earthobservatory.nasa.gov/> (accessed 4.3.23).

Rice, J., Wutich, A., Westerhoff, P., 2013. Assessment of De Facto Wastewater Reuse across the U.S.: Trends between 1980 and 2008. *Environ. Sci. Technol.* 47, 11099–11105. <https://doi.org/10.1021/es402792s>.

Rode, M., Wade, A.J., Cohen, M.J., Hensley, R.T., Bowes, M.J., Kirchner, J.W., Arhonditsis, G.B., Jordan, P., Kronvang, B., Halliday, S.J., Skeffington, R.A., Rozemeijer, J.C., Aubert, A.H., Rinke, K., Jomaa, S., 2016. Sensors in the Stream: The High-Frequency Wave of the Present. *Environmental Science & Technology* 50, 10297–10307. <https://doi.org/10.1021/acs.est.6b02155>.

Rup, 2006. *Processes of transferring pollutants in the natural environment*. Scientific and Technical Publishing House, Warsaw.

Rutherford, 1994. River Mixing - Rutherford, J. C.: 9780471942825 - AbeBooks [WWW Document]. URL <https://www.abebooks.com/9780471942825/River-Mixing-Rutherford-J-C-0471942820/plp> (accessed 5.22.23).

Skorbiotowicz, M., Skorbiotowicz, E., Wójcikowicz, P., Zamojska, E., 2017. DETERMINATION OF MIXING ZONES FOR WASTEWATER WITH RECEIVER WATERS. *J. Ecol. Eng.* 18, 192–198. <https://doi.org/10.12911/22998993/74291>.

Summers, B.M., Horn, D.J.V., González-Pinzón, R., Bixby, R.J., Grace, M.R., Sherson, L.R., Crossey, L.J., Stone, M.C., Parmenter, R.R., Compton, T.S., Dahm, C.N., 2020. Long-term data reveal highly-variable metabolism and transitions in trophic status in a montane stream. *Freshwater Science* 39, 241–255. <https://doi.org/10.1086/708659>.

Tiwari, B., Sellamuthu, B., Ouarda, Y., Drogui, P., Tyagi, R.D., Buelna, G., 2017. Review on fate and mechanism of removal of pharmaceutical pollutants from wastewater using biological approach. *Bioresource Technology* 224, 1–12. <https://doi.org/10.1016/j.biortech.2016.11.042>.

UNESCO, 2020. United Nations World Water Development Report 2020 [WWW Document]. URL <https://unesdoc.unesco.org/ark:/48223/pf0000372985/PDF/372985eng.pdf.multi> (accessed 3.3.22).

United Nations Environment Programme, 2021. The United Nations World Water Development Report 2021: Valuing Water. UNESCO, Paris. [WWW Document]. URL <https://unesdoc.unesco.org/ark:/48223/pf0000375724/PDF/375724eng.pdf.multi> (accessed 4.3.23).

Wang, H., Xi, H., Xu, L., Jin, M., Zhao, W., Liu, H., 2021. Ecotoxicological effects, environmental fate and risks of pharmaceutical and personal care products in the water environment: A review. *Science of the Total Environment* 788, 147819. <https://doi.org/10.1016/j.scitotenv.2021.147819>.

Ward, P.R.B., 1973. Prediction of Mixing Lengths for River Flow Gaging. *Journal of the Hydraulics Division* 99, 1069–1081. <https://doi.org/10.1061/JYCEAJ.0003677>.

Zavalá, C., 2020. Hyperpycnal (over density) flows and deposits. *Journal of Palaeogeography* 9, 17. <https://doi.org/10.1186/s42501-020-00065-x>.